Journal of the Korean Ceramic Society
Vol. 45, No. 5, pp. 251~255, 2008.

Effects of Crystal Structure on Microwave Dielectric Properties of Ceramics

Eung Soo Kim†, Chang Jun Jeon, Sung Joo Kim, and Su Jung Kim

Department of Materials Engineering, Kyonggi University, Suwon 443-760, Korea
(Received April 24, 2008; Accepted May 8, 2008)

ABSTRACT

Microwave dielectric properties of $MgTiO_3$, $MgWO_4$, $MgNb_2O_6$, and $MgTa_2O_6$ were investigated based on the structural characteristics. The dielectric constant (K) was dependent on the dielectric polarizabilities of the specimens, and the deviation of the observed dielectric polarizabilities ($\alpha_{obs.}$) from the theoretical dielectric polarizabilities ($\alpha_{theo.}$) were decreased with increasing of Mg-site bond valence. Quality factors (Qf) were affected by the sharing type of MgO_6 and BO_6 octahedra. Temperature coefficient of resonant frequency (TCF) was decreased with increasing of average octahedral distortion.

Key words : Microwave dielectric properties, Octahedral distortion, Dielectric polarizabilities, Bond valence

1. Introduction

With the rapid growth of the wireless communication industry, tailoring the microwave dielectric properties of ceramics has been widely studied for high-performance materials suitable to wireless applications. However, most studies in this field have been focused on improving the microwave dielectric properties through various experiments. Therefore, the dependence of microwave dielectric properties on composition and crystal structure should be studied to predict and control effectively the microwave dielectric properties of ceramics.

Microwave dielectric properties are largely dependent on the structural characteristics of materials. In particular, the temperature coefficient of resoanant frequency (TCF) is closely related to the distortion of oxygen octahedra resulting from the changes of bond length between the octahedral cation and oxygen ion,[1] while the quality factor (Qf) is affected by the sharing type of oxygen octahedra.[2] The dielectric constant (K) is dependent not only on the dielectric polarizabilities of the composing ions of the compound, but also on the rattling or compression effect of the octahedral cation resulting from the changes of bond valence between the octahedral cation and oxygen ion.[3]

In general, Mg-based ceramics, such as $MgTiO_3$, $MgWO_4$, $MgNb_2O_6$, and $MgTa_2O_6$ have Mg- and B-site oxygen octahedra composed of the octahedral cation with six oxygen ions. Even though the difference of the B-site ionic size (Ti^{4+}=0.605 Å, W^{6+}=0.6 Å, Nb^{5+}= 0.64 Å, Ta^{5+}=0.64 Å) is not much at the coordination number of 6,[4] the crystal structure of these Mg-based ceramics was distinguished from the sharing type of MgO_6 and BO_6 octahedra, unit-cell volume, and bond valence between octahedral cation and oxygen ion.

Therefore, the microwave dielectric properties of $MgTiO_3$, $MgWO_4$, $MgNb_2O_6$, and $MgTa_2O_6$ ceramics were investigated with regard to the crystallographic considerations of oxygen octahedra.

2. Experimental Procedure

Oxide powders with purity above 99.9% were used as starting materials. The powders were weighed according to the compositions of $MgTiO_3$, $MgWO_4$, $MgNb_2O_6$, and $MgTa_2O_6$, and then milled with ZrO_2 balls in ethanol for 24 h. To obtain a single phase of each composition, $MgWO_4$ was calcined at 700°C for 3 h, while $MgTiO_3$, $MgNb_2O_6$, and $MgTa_2O_6$ were calcined at 1100°C for 3 h, respectively. These calcined powders were re-milled for 24 h, and pressed into pellets isostatically under the pressure of 1500 kg/cm^2. These pellets were sintered from 1100°C to 1400°C for 3 h in air.

Powder X-ray diffraction analysis (D/Max-3C, RIGAKU, Japan) was used to determine the crystalline phases. From the Rietveld refinements of X-ray diffraction (XRD) patterns, the atomic positions, lattice parameters, and unit cell volumes of the sintered specimens were obtained using a Rietan-2000 program.[5] The micro- structure of the sintered specimens was observed via scanning electron microscope (SEM, JSM-6700F, JEOL, Japan). The dielectric constant (K) and unloaded Q value at 9~11 GHz were measured by the Hakki and Coleman method.[6] The temperature coefficient of the resonant frequency (TCF) was measured by the cavity method[7] in the temperature range from 20°C to 80°C.

†Corresponding author : Eung Soo Kim
E-mail : eskim@kyonggi.ac.kr
Tel : +82-31-249-9764 Fax : +82-31-244-6300

Table 1. Sintering Temperature and Density of $MgTiO_3$, $MgWO_4$, $MgNb_2O_6$, and $MgTa_2O_6$ Sintered Specimens

Compound	Sintering temperature (°C)	Apparent density (g/cm^3)	Relative density (%)
$MgTiO_3$	1400	3.78	97.05
$MgWO_4$	1100	6.58	95.46
$MgNb_2O_6$	1350	4.84	96.85
$MgTa_2O_6$	1350	7.45	95.32

3. Results and Discussion

The optimal sintering temperature of $MgTiO_3$, $MgWO_4$, $MgNb_2O_6$, and $MgTa_2O_6$ ceramics (Mg-based ceramics) changed with the type of B-site cations used (B=Ti^{4+}, W^{6+}, Nb^{5+}, Ta^{5+}), as summarized in Table 1. To reduce the effects of density on the microwave dielectric properties, the relative density was above 95% of theoretical density of each composition.

As shown in Fig. 1, Mg-based ceramics showed the single phase with their own crystal structures: trigonal ilmenite for $MgTiO_3$, monoclinic wolframite for $MgWO_4$, orthorhombic columbite for $MgNb_2O_6$, and tetragoral tri-rutile for $MgTa_2O_6$, respectively. The refined atomic positions and lattice parameters of the sintered specimens obtained from the Rietveld refinement are shown in Table 2. For the Mg-based ceramics, the coordination number of Mg- and B-site cations is six, and MgO_6 octahedra are connected to BO_6 octahedra with their own sharing type (corner, edge, face) of octahedra in the unit cell. Although the difference of the B-site ionic size (Ti^{4+}=0.605 Å, W^{6+}=0.6 Å, Nb^{5+}=0.64 Å, Ta^{5+}=0.64 Å)[4] is not much, the unit cell volume changed remarkably with the type of B-site cations used due to the changes of crystal structure.

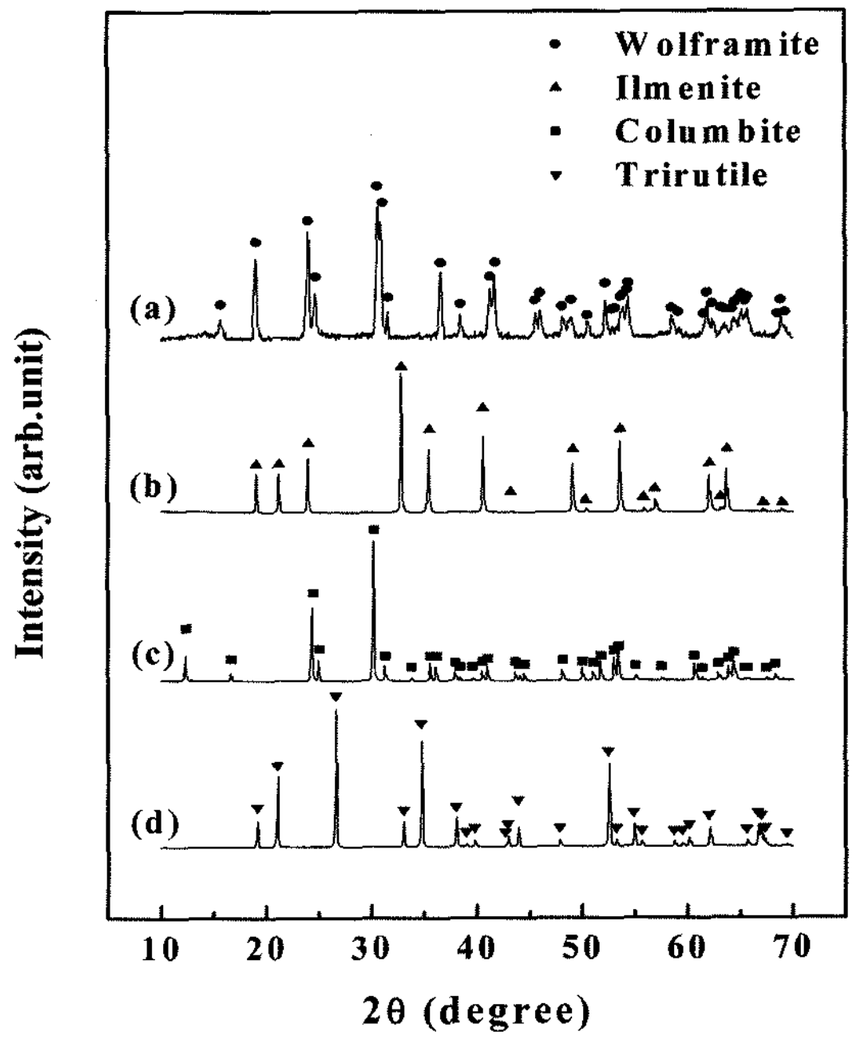

Fig. 1. X-ray diffraction patterns of (a) $MgWO_4$, (b) $MgTiO_3$, (c) $MgNb_2O_6$, and (d) $MgTa_2O_6$ sintered specimens.

These results could be attributed to the differences of the bond strength resulting from the sharing type of MgO_6 and BO_6 octahedra. The bond strength between an octahedral cation and an oxygen ion was closely related with the bond valence, which is a function of the bond length and bond valence parameter.[8] Therefore, the bond valence could be applied to the estimation of bond strength. The bond valences between a Mg^{2+} cation and an oxygen ion, $v_{Mg\text{-}O}$ were calculated from eq. (1).[9]

Table 2. Atomic Positions and Lattice Parameters of $MgTiO_3$, $MgWO_4$, $MgNb_2O_6$, and $MgTa_2O_6$ Sintered Specimens

Compound	Space group	Atom	Wyckoff site	x	y	z	Occupation	Lattice parameters (Å)		
								a	b	c
$MgTiO_3$	*R-3H*	Mg	6c	0	0	0.356	1.0	5.054	5.054	13.942
		Ti	6c	0	0	0.145	1.0			
		O	18f	0.316	0.022	0.246	1.0			
$MgWO_4$	*P12/c1*	Mg	2f	0.500	0.672	0.250	1.0	4.624	5.594	4.880
		W	2e	0	0.183	0.250	1.0			
		O_1	4g	0.219	0.107	0.938	1.0			
		O_2	4g	0.255	0.382	0.402	1.0			
$MgNb_2O_6$	*Pbcn*	Mg	4c	0	0.169	0.250	1.0	5.703	14.199	5.037
		Nb	8d	0.160	0.318	0.754	1.0			
		O_1	8d	0.096	0.394	0.432	1.0			
		O_2	8d	0.080	0.116	0.907	1.0			
		O_3	8d	0.256	0.122	0.583	1.0			
$MgTa_2O_6$	$P4_2/mnm$	Mg	2a	0	0	0	1.0	4.718	4.718	9.212
		Ta	4e	0	0	0.332	1.0			
		O_1	4f	0.309	0.309	0	1.0			
		O_2	8j	0.298	0.298	0.324	1.0			

Table 3. Mg-site Bond Valence (V_{Mg}) of $MgTiO_3$, $MgWO_4$, $MgNb_2O_6$, and $MgTa_2O_6$ Sintered Specimens

Compound	$R_{Mg\text{-}O}$ (Å)	$d1_{Mg\text{-}O}$ (Å)	$d2_{Mg\text{-}O}$ (Å)	$d3_{Mg\text{-}O}$ (Å)	$v1_{Mg\text{-}O}$	$v2_{Mg\text{-}O}$	$v3_{Mg\text{-}O}$	V_{Mg}
$MgWO_4$	1.693	2.174(×2)	2.053(×2)	2.094(×2)	0.273(×2)	0.378(×2)	0.338(×2)	1.977
$MgTiO_3$	1.693	2.163(×3)	2.043(×3)		0.281(×3)	0.388(×3)		2.007
$MgNb_2O_6$	1.693	2.080(×4)	2.132(×2)		0.351(×4)	0.305(×2)		2.016
$MgTa_2O_6$	1.693	2.117(×4)	2.052(×2)		0.318(×4)	0.379(×2)		2.030

Table 4. Comparison of Observed and Theoretical Polarizabilities of $MgTiO_3$, $MgWO_4$, $MgNb_2O_6$, and $MgTa_2O_6$ Sintered Specimens

Compound	Theoretical	Observed				Δ %
	$\alpha_{theo.}$(Å^3)	K	$V_{unitcell}$(Å^3)	Z	$\alpha_{obs.}$(Å^3)	$(\alpha_{obs.}-\alpha_{theo.})/\alpha_{obs.}\times 100$
$MgWO_4$	9.46	12.44	131.10	2	12.3978	23.6959
$MgTiO_3$	10.28	18.45	307.91	6	10.4541	1.6653
$MgNb_2O_6$	21.32	20.84	407.83	4	21.1435	−0.8349
$MgTa_2O_6$	22.84	25.48	205.06	2	21.8051	−4.7464

$$v_{Mg-O} = exp\left[\frac{(R_{Mg-O}-d_{Mg-O})}{b}\right] \quad (1)$$

where $R_{Mg\text{-}O}$ is the bond valence parameter, $d_{Mg\text{-}O}$ is the bond length between Mg^{2+} and oxygen ions, and b is commonly taken to be a universal constant equal to 0.37 Å.[10] The bond valence parameters followed the values in a previous report.[9] The Mg-site bond valence (V_{Mg}) was defined as the sum of all the valences from a given Mg^{2+} cation, and was calculated from eq. (2).[9]

$$V_{Mg} = \sum_{O} v_{Mg-O} \quad (2)$$

Table 3 summarizes the V_{Mg} of Mg-based ceramics. The V_{Mg} of the specimens increased with the type of B-site cations used (B = W^{6+}, Ti^{4+}, Nb^{5+}, Ta^{5+}).

At microwave frequencies, the dielectric constant (K) is not only dependent on the density and secondary phases, but also on the crystal structure.[12] Since the relative density was higher than 95% (Table 1) and there was no secondary phase (Fig. 1) in the given compositions, the K was not significantly affected by the relative density or a secondary phase.

Effects of crystal structure on the dielectric constant (K) could be evaluated by the comparisons between the theoretical dielectric polarizabilities ($a_{theo.}$) obtained from the additive rule[11] and the observed dielectric polarizabilities ($a_{obs.}$) obtained from the measured K using the Clauses - Mosotti equation.[11]

Table 4 shows the comparisons of $a_{theo.}$ and $a_{obs.}$ of the Mg-based ceramics. Both $a_{theo.}$ and $a_{obs.}$ were dependent on the dielectric constant (K) of each composition; however, the deviations of $a_{obs.}$ from $a_{theo.}$ changed with the type of B-site

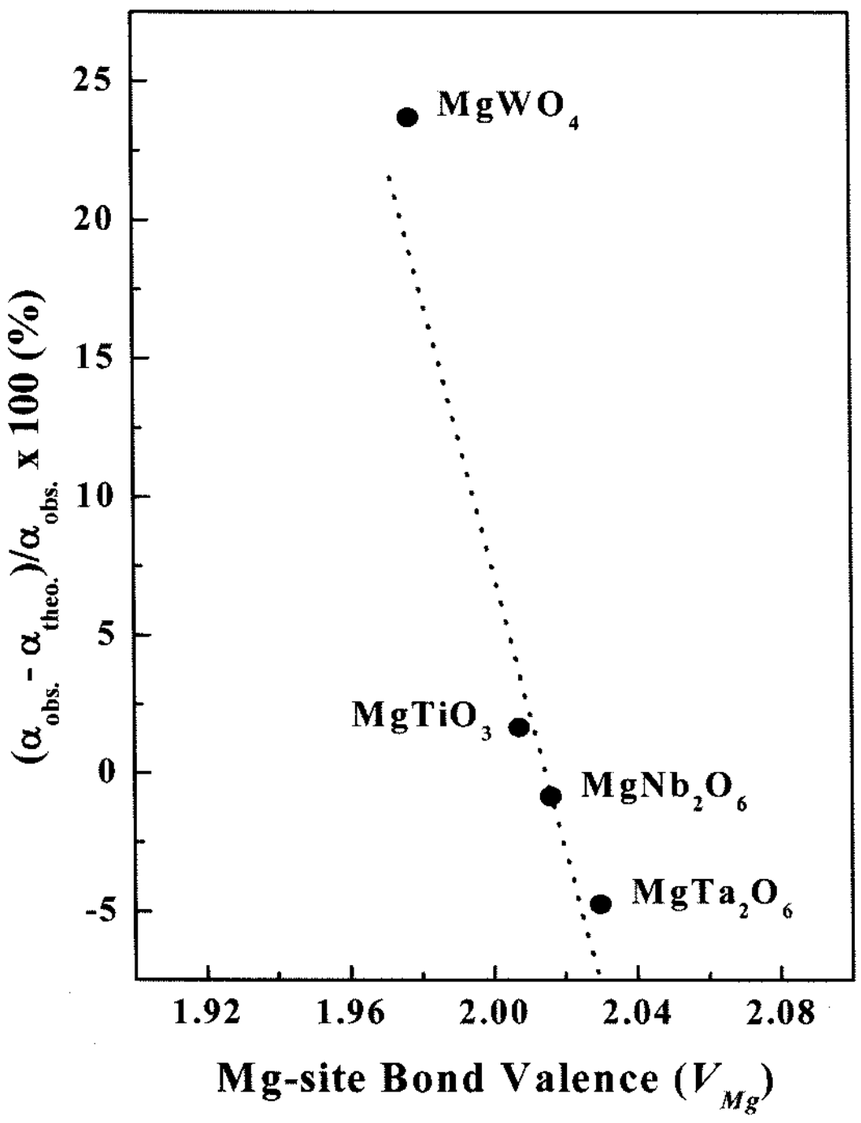

Fig. 2. Dependence of polarizabilities deviations on Mg-site bond valence (V_{Mg}) of Mg-based ceramics.

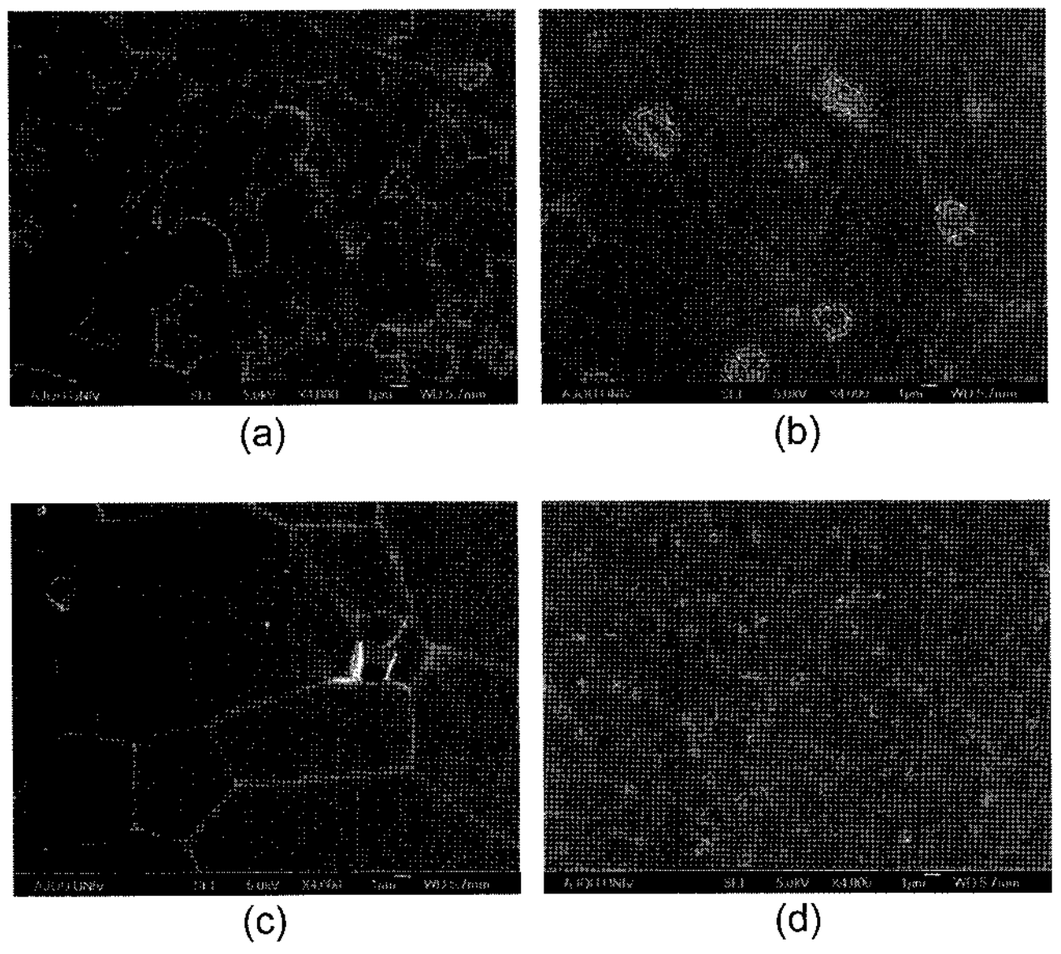

Fig. 3. SEM micrographs of (a) $MgWO_4$, (b) $MgTiO_3$, (c) $MgNb_2O_6$, and (d) $MgTa_2O_6$ sintered specimens.

Table 5. *Qf* Value and Sharing Type of MgO_6 and BO_6 Octahedra of $MgTiO_3$, $MgWO_4$, $MgNb_2O_6$, and $MgTa_2O_6$ Sintered Specimens

Compound	*Qf* (GHz)	Crystal structure	Sharing type of MgO_6 and BO_6 octahedra
$MgTiO_3$	369,118	Ilmenite	Face
$MgTa_2O_6$	166,032	Tri-rutile	Edge
$MgNb_2O_6$	108,882	Columbite	Corner
$MgWO_4$	23,068	Wolframite	Corner

cations (B=W^{6+}, Ti^{4+}, Nb^{5+}, Ta^{5+}). These results could be attributed to the Mg-site bond valence (V_{Mg}), shown in Table 3, which resulted from the crystal structure of each composition. Fig. 2 shows the dependence of polarizabilities deviations on V_{Mg}. With the increase of V_{Mg}, the rattling of an octahedral cation (Mg^{2+}) decreased; in turn, the $a_{obs.}$ decreased. Therefore, K of the specimens was strongly dependent on the dielectric polarizabilities of composition.

It has been reported[13] that the *Qf* value depends on intrinsic factors, such as crystal structure and lattice vibrations, as well as on extrinsic factors, such as density, secondary phase, and grain size. The effect of extrinsic factors on *Qf* value could be negligible due to a relative density of higher than 95% (Table 1) and no secondary phase (Fig. 1).

As shown in Fig. 3, the grain size of the $MgNb_2O_6$ specimen was larger than the $MgTiO_3$, $MgWO_4$, and $MgTa_2O_6$ specimens. However, the *Qf* value of $MgNb_2O_6$ was smaller than those of $MgTiO_3$ and $MgTa_2O_6$. Therefore, the relationship between the crystal structure and *Qf* value of Mg-based ceramics should be considered. The *Qf* value of $MgTiO_3$ (ilmenite) was remarkably larger than those of $MgTa_2O_6$ (tri-rutile), $MgNb_2O_6$ (columbite), and $MgWO_4$ (wolframite). The face sharing of MgO_6 and BO_6 octahedra has a larger

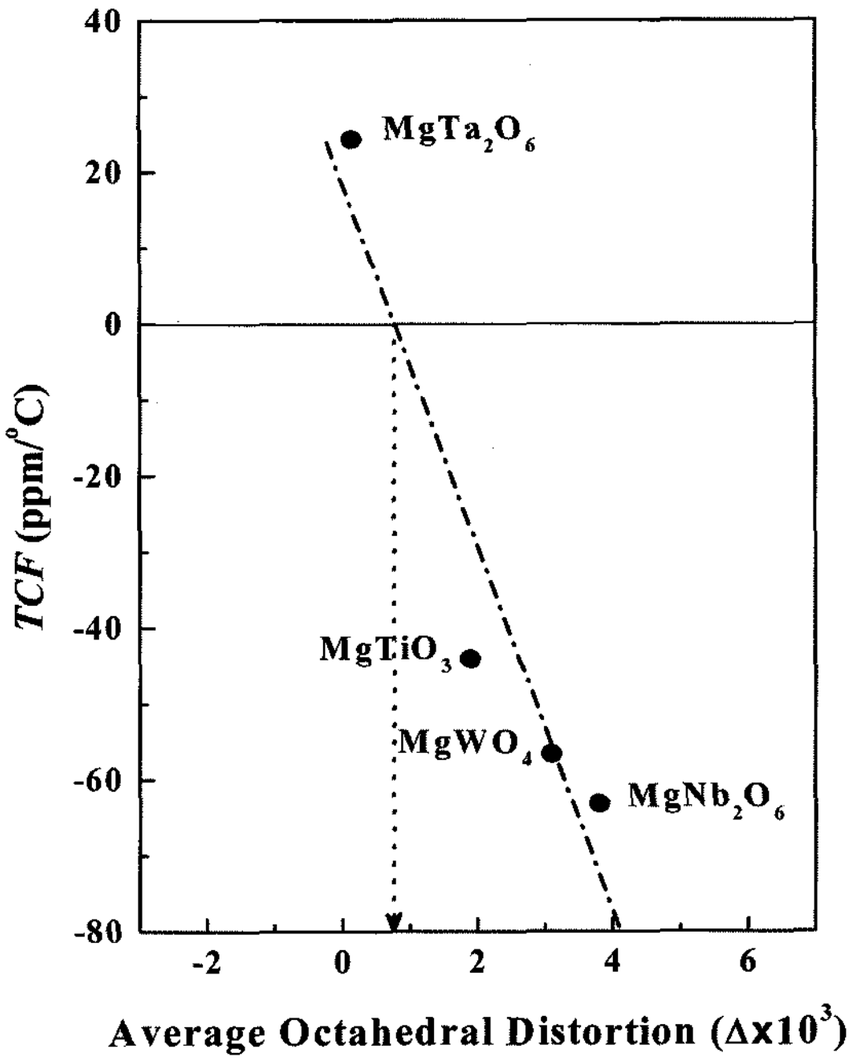

Fig. 4. Dependence of *TCF* on the octahedral distortions of Mg-based ceramics.

Table 6. Average Octahedral Distortion and *TCF* of $MgTiO_3$, $MgWO_4$, $MgNb_2O_6$, and $MgTa_2O_6$ Sintered Specimens

	Compound			
	$MgTa_2O_6$	$MgTiO_3$	$MgWO_4$	$MgNb_2O_6$
$R1_{Mg\text{-}O}$(Å)	2.117(×4)	2.163(×3)	2.174(×2)	2.080(×4)
$R2_{Mg\text{-}O}$(Å)	2.052(×2)	2.043(×3)	2.053(×2)	2.132(×2)
$R3_{Mg\text{-}O}$(Å)			2.094(×2)	
Average $R_{Mg\text{-}O}$(Å)	2.085	2.103	2.107	2.106
$R1_{B\text{-}O}$(Å)	1.964(×2)	2.098(×3)	1.911(×2)	1.908
$R2_{B\text{-}O}$(Å)	2.007(×2)	1.881(×3)	1.781(×2)	2.070
$R3_{B\text{-}O}$(Å)	1.980(×2)		2.134(×2)	1.959
$R4_{B\text{-}O}$(Å)				2.272
$R5_{B\text{-}O}$(Å)				2.080
$R6_{B\text{-}O}$(Å)				1.794
Average $R_{B\text{-}O}$(Å)	1.984	1.990	1.942	2.014
Mg-site octahedral distortion ($\Delta_{Mg}\times10^3$)	0.243	0.814	0.566	0.152
B-site octahedral distortion ($\Delta_B\times10^3$)	0.080(×2)	2.971	5.617	5.619(×2)
Average octahedral distortion ($\Delta\times10^3$)	0.134	1.893	3.091	3.797
TCF (ppm/°C)	24.35	−44.07	−56.6	−63.17

sharing area than the edge or corner sharing of MgO_6 and BO_6 octahedra. With the increase of sharing area of MgO_6 and BO_6, the *Qf* value of the specimens increased, as shown in Table 5. Therefore, the *Qf* value of the specimens was affected by the sharing type of MgO_6 and BO_6 octahedra. Even though $MgNb_2O_6$ and $MgWO_4$ show the same corner sharing of MgO_6 and BO_6 octahedra, the *Qf* value of $MgNb_2O_6$ was larger than that of $MgWO_4$. The reasons why $MgNb_2O_6$ showed a larger *Qf* value than that of $MgWO_4$ may be related to the Mg-site bond valence but are, as yet, unclear and under investigation.

Table 6 summarizes the average octahedral distortion and the temperature coefficient of resonant frequency (*TCF*) of the Mg-based ceramics. The individual bond lengths of oxygen octahedra were obtained from the atomic positions and lattice parameters, as confirmed in Table 2. From the individual bond length of the oxygen octahedra, the octahedral distortion (D) of all the structures was calculated from eq. (3).[4)]

$$\Delta = \frac{1}{6}\sum\left\{\frac{(R_i - \overline{R})}{\overline{R}}\right\}^2 \quad (3)$$

where R_i is an individual bond length, and $\overline{R}$ is the average bond length of oxygen octahedra. With the type of B-site cations (B=Ta^{5+}, Ti^{4+}, W^{6+}, Nb^{5+}), the *TCF* of the specimens decreased due to the increase of average octahedral distortion, as shown in Fig. 4. A *TCF* of zero could be obtained by the control of the average octahedral distortion of ceramics resulting from the substitution of ions with ionic sizes between 0.605 Å (Ti^{4+}) and 0.64 Å (Ta^{5+}) for the B-site of Mg-based ceramics.

4. Conclusions

For $MgTiO_3$, $MgWO_4$, $MgNb_2O_6$, and $MgTa_2O_6$ ceramics, a single phase with trigonal ilmenite (B=Ti^{4+}), monoclinic wolframite (B= W^{6+}), orthorhombic columbite (B=Nb^{5+}) and tetragonal tri-rutile (B= Ta^{5+}) structures were confirmed, respectively.

The dielectric constant (*K*) was largely dependent on the dielectric polarizabilities of composition. The deviation of the observed dielectric polarizabilities ($a_{obs.}$) from the theoretical dielectric polarizabilities ($a_{theo.}$) decreased with increasing Mg-site bond valence. The quality factor (*Qf*) value of $MgTiO_3$ was remarkably larger than those of $MgTa_2O_6$, $MgNb_2O_6$, and $MgWO_4$. These results could be attributed to the sharing area of MgO_6 and BO_6 octahedra. With the type of B-site cations (B=Ta^{5+}, Ti^{4+}, W^{6+}, Nb^{5+}), the temperature coefficient of resonant frequency (*TCF*) of the specimens decreased with increasing average octahedral distortion.

Acknowledgements

This work was supported by a Kyonggi University Research Grant, 2007.

REFERENCES

1. E. S. Kim, S. H. Kim, and K. H. Yoon, "Dependence of Thermal Stability on Octahedral Distortion of (1-x)$(Ca_{0.3}Li_{0.119}Sm_{0.427})TiO_3$-x$LnAlO_3$ (Ln=Nd, Sm) Ceramics," *J. Ceram. Soc. Jpn.*, **112** 1645-49 (2004).
2. J. H. Shon, Y. Inaguma, S. O. Yoon, M. Itoh, T. Nakamura, S. J. Yoon, and H. J. Kim, "Microwave Dielectric Characteristics of Ilmenite-Type Titanates with High Q Values," *Jpn. J. Appl. Phys.*, **33** 5466-70 (1994).
3. E. S. Kim and K. H. Yoon, "Microwave Dielectric Properties of (1-x)$CaTiO_3$-x$Li_{1/2}Sm_{1/2}TiO_3$ Ceramics," *J. Euro. Ceram. Soc.*, **23** 2397-401 (2003).
4. R. D. Shannon, "Revised Effective Ionic Radii and Systematic Studies of Interatomic Distances in Halides and Chalcogenides," *Acta Cryst.*, **A32** 751-67 (1976).
5. F. Izumi and T. Ikeda, "A Rietveld-Analysis Programm RIETAN-98 and its Applications to Zeolites," *Mater. Sci. Forum*, **321** 198-203 (2000).
6. B. W. Hakki and P. D. Coleman, "A Dielectric Resonator Method of Measuring Inductive Capacities in the Millimeter Range," *IRE Trans. Microwave Theory Tech.*, **8** 402-10 (1960).
7. T. Nishikawa, K. Wakino, H. Tamura, H. Tanaka, and Y. Ishikawa, "Precise Measurement Method for Temperature Coefficient of Microwave Dielectric Resonator Material," *IEEE MTT-S Int. Microwave Symp. Dig.*, 277-80 (1987).
8. H. S. Park, K. H. Yoon, and E. S. Kim, "Relationship between the Bond Valence and the Temperature Coefficient of the Resonant Frequency in the Complex Perovskite $(Pb_{1-x}Ca_x)[Fe_{0.5}(Nb_{1-y}Ta_y)_{0.5}]O_3$," *J. Am. Ceram.* Soc., **84** 99-103 (2001).
9. N. B. Brese and M. O'Keefe, "Bond-Valence Parameters for Solids," *Acta Cryst.*, **B47** 192-97 (1991).
10. I. D. Brown and D. Altermatt, "Bond-Valence Parameters Obtained from a Systematic Analysis of the Inorganic Crystal Structure Database," *Acta Cryst.*, **B41** 244-47 (1985).
11. R. D. Shannon, "Dielectirc Polarizabilities of Ions in Oxides and Fluorides," *J. Appl. Phys.*, **73** 348-66 (1993).
12. D. M. Iddles, A. J. Bell, and A. J. Moulson, "Relationships between Dopants, Microstructure and the Microwave Dielectric Properties of ZrO_2-TiO_2-SnO_2 Ceramics." *J. Mater. Sci.*, **27** 6303-07 (1992).
13. S. G. Mhaisalkar, D. W. Readey, S. A. Akbar, P. K. Dutta, M. J. Sumnar, and R. Rokhlin, "Infrared Reflectance Spectra of Doped $BaTi_4O_9$." *J. Solid State Chem.*, **95** 275-82 (1991).